Inorg. Chem. **2009**, *48*, 496−507

Discrete Polyoxovanadate Cluster into an Organic Free Metal-Oxide-Based Material: Syntheses, Crystal Structures, and Magnetic Properties of a New Series of Lanthanide Linked-POV Compounds $[\{Ln(H_2O)_6\}_2As_8V_{14}O_{42}(SO_3)]\cdot 8H_2O$ (Ln = La^{3+}, Sm^{3+}, and Ce^{3+})†

T. Arumuganathan and Samar K. Das*

School of Chemistry, University of Hyderabad, Hyderabad 500 046, India

Received February 7, 2008

This article describes the linking propensity of the sulfite encapsulated polyoxovanadate (POV) anion, $[As_8V_{14}O_{42}(SO_3)]^{6-}$, with aqua−lanthanide complex cations $[Ln(H_2O)_6]^{3+}$ in a controlled wet synthesis resulting in a series of organic free metal-oxide-based materials $[\{Ln(H_2O)_6\}_2As_8V_{14}O_{42}(SO_3)]\cdot 8H_2O$, Ln = La^{3+} (**1**), Sm^{3+} (**2**), and Ce^{3+} (**3**). The title compounds have been characterized by elemental analyses, IR, diffuse reflectance, electron paramagnetic resonance, powder X-ray diffraction (XRD), thermogravimetric analysis (TGA), and single-crystal X-ray diffraction studies. All three compounds crystallize in the monoclinic space group $P2_1/n$. Crystal data for **1**: a = 13.4839(7), b = 12.3388(6), c = 18.3572(10) Å, β = 108.2570 (10)°, V = 2900.4(3) Å^3. Crystal data for **2**: a = 13.4156(3), b = 12.2588(3), c = 18.2501(4) Å, β = 108.049(3)°, V = 2853.8(10) Å^3. Crystal data for **3**: a = 13.4934(3), b = 12.3983(3), c = 18.3992(4) Å, β = 108.025 (3), V = 2927.0(10) Å^3. Crystal structure shows that each cluster is surrounded by six $[Ln(H_2O)_6]^{3+}$ complex cations, and each $[Ln(H_2O)_6]^{3+}$ cation is coordinated to three surrounding POV cluster anions. The electron spin resonance spectra of compounds **1**−**3** show a typical single line (g = 1.9671 for **1**, g = 1.9669 for **2**, and g = 1.9704 for **3**), characteristic for a V^{4+} (d^4) ion; in addition, a supplementary signal appears for compound **2** at g = 5.9238 due to the presence of the Sm^{3+} (f^5) ion. All vanadium atoms exit in +4 oxidation states that have been confirmed by bond valence sum calculations. Variable-temperature magnetic studies for all three compounds **1**−**3** are performed and are discussed in terms of antiferromagnetic coupling interactions, giving importance to linking/assembling the $\{V_{14}\}$ cluster anions. TGA/mass analyses of compounds **1**−**3** (linked system) have been compared with that of the starting precursor $[NH_4]_6[As_8V_{14}O_{42}(SO_3)]$ (discrete building unit). Interestingly, the evolution of SO_2 gas takes place for the discrete cluster compound $[NH_4]_6[As_8V_{14}O_{42}(SO_3)]$ in a temperature range of 480−520 °C with the decomposition of the POV cluster anion, whereas the same evolution occurs at 520−580 °C for compounds **1**−**3**. These comparative TGA/mass studies help to understand how the organic free linker elevates the thermal stability of the sulfite encapsulated POV cluster anion in going from a discrete cluster anion to the linked system (molecule to material). It has also been demonstrated that the stability of the sulfite anion increases to a greater extent when it is included in the cluster cage. The powder XRD studies of compounds **1**−**3** confirm that these are isostructural materials and provide information about the phase purity.

Introduction

The synthesis of novel materials with interesting physical and chemical properties, especially toward magnetic, electronic, and conductive applications, is a challenging task in modern inorganic chemistry.[1] These materials may be constructed either by supramolecular or covalent interactions using a well-defined building block. A minimum criterion/requirement for a molecule to become a material is its stability toward external stimulus factors, for example, light, heat, and so forth. Thermal stability for a material is of prime importance, because practical applications (e.g., host guest properties, catalysis, sensing) require elevated temperatures

† Dedicated to Eminent Professor C. N. R. Rao on the occasion of his 75th birthday.

* Author to whom correspondence should be addressed. E-mail: skdsc@uohyd.ernet.in.

10.1021/ic8002383 CCC: $40.75
Published on Web 12/18/2008

in most cases. To achieve a considerable thermal stability, meaningful contacts and connections are essential in this approach of "molecule to material". Polyoxometalate (POM) clusters have been proved to be potential building units to obtain a range of materials of numerous applications in the field of materials chemistry.[2] This is because POMs are generally metal-oxide-based clusters that can be generated simply from an aqueous solution and have well-defined topologies.[3] Indeed, how a POM cluster/molecule goes to a material is a major subject of research in modern materials chemistry, and numerous publications have appeared in this regard in recent time.[4] Polyoxovanadates (henceforth, POVs) comprise an important class of POMs that have received considerable attention because of their diverse topologies, structural and electronic properties, and versatile industrial applications, for example, in catalysis and materials science (e.g., as cathodes in lithium batteries).[5] The catalysis, driven by the POVs, is accelerated by the facile change of oxidation states of the vanadium center (V^V can be converted to V^{IV} and vice versa). Among POVs, a major subclass is the V/As/O heteropoly system that is not as explored as is the V−O or V−P−O system.[6] In general, the V/As/O heteropoly system can be divided into five different groups based on the number of As and V atoms present in these clusters:[7] (i) $[As_6V_{15}O_{42}]^{n-}$, (ii) $[As_8V_{14}O_{42}]^{n-}$, (iii) $[As_8V_{12}O_{40}]^{n-}$, (iv) $[As_2V_{10}O_{26}]^{n-}$, and (v) $[As_8V_6O_{26}]^{n-}$. Compounds of the (i) and (ii) types are extremely popular as far as magnetic materials are concerned. Investigations of magnetic properties of these compounds (V15 and V14) have demonstrated how magnetic susceptibility and electron paramagnetic resonance spectra can allow a reasonably detailed understanding of the preferred spin arrangement in high nuclearity spin clusters using variable-temperature parameters.[8] It was discussed that these compounds should mimic the properties of bulk magnets. We have chosen a well-studied sulfite anion encapsulated POV cluster $[As_8V_{14}O_{42}(SO_3)]^{6-}$ as a building block and explored its linking propensity toward the lanthanide cations. In fact, this cluster anion has been used as a potential building unit in constructing coordination polymers using metal-organic complexes as linkers.[9] Since our intention is to achieve a stable material from this POV cluster, we intended to avoid "metal-coordination complexes with organic ligands" as linkers and connectors. This is because organic moieties are susceptible to decomposing or burning at higher temperatures (in the temperature range

(1) (a) *Molecular Electronics Devices I*; Carter, F. L., Ed.; Dekker: New York, 1982; p 1987. (b) Topical issue on polyoxometalates: Hill, C. L. *Chem. Rev* **1998**, *98*, 1–389. (c) *Polyoxometalate Chemistry for Nano-Composite Design*; Yamase, T., Pope, M. T., Eds.; Nanostructure Science and Technology, Kluwer Academic/Plenum Publishing: New York, 2002. (d) *Polyoxomatalates: From Platonic Solids to Anti-Retroviral Activity*; Pope, M. T., Müller, A., Eds.; Kluwer: Dordrecht, The Netherlands, 1993. (e) Pope, M. T. *Comp. Coord. Chem. II* **2003**, *4*, 635. (f) *Polyoxometalate Molecular Science*; Borràs-Almenar, J. J., Coronado, E., Müller, A., Pope, M. T., Eds.; Kluwer: Dordrecht, The Netherlands, 2003. (g) Chen, L.; Jiang, F.; Lin, Z.; Zhou, Y.; Yue, C.; Hong, M. *J. Am. Chem. Soc.* **2005**, *127*, 8588. (h) Zarembowitch, J.; Kahn, O. *New. J. Chem.* **1991**, *15*, 181.

(2) (a) Müller, A.; Peters, F.; Pope, M. T.; Gatteschi, D. *Chem. Rev.* **1998**, *98*, 239. (b) Coronado, E.; Giménez-Saiz, C.; Gómez-García, C. J. *Coord. Chem. Rev.* **2005**, *249*, 1776, and references cited therein.

(3) (a) Pope, M. T. *Heteropoly and Isopoly Oxometalates*; Springer-Verlag: Berlin, 1983. (b) Khan, M. I.; Ayesh, S.; Doedens, R. J.; Yu, M. H.; O'Connor, C. J. *Chem. Commun.* **2005**, 4658.

(4) (a) Soghomonian, V.; Chen, Q.; Haushalter, R. C.; Zubieta, J.; O'Connor, C. J. *Science* **1993**, *25*, 1596. (b) Hagrman, D.; Hagrman, P. J.; Zubieta, J. *Angew. Chem., Int. Ed. Engl.* **1999**, *38*, 3165. (c) Hagrman, P. J.; Zubieta, J. *Inorg. Chem.* **2000**, *39*, 3252. (d) Hagrman, D.; Sangregorio, C.; O'Connor, C. J.; Zubieta, J. *J. Chem. Soc., Dalton Trans.* **1998**, 3707. (f) Hagrman, P. J.; Hagrman, D.; Zubieta, J. *Angew. Chem., Int. Ed. Engl.* **1999**, *38*, 2638. (g) Khan, M. I. *J. Solid State Chem.* **2000**, *152*, 105. (h) Khan, M. I.; Yohannes, E.; Powell, D. *Chem. Commun.* **1999**, 23. (i) Khan, M. I.; Yohannes, E.; Dödens, D. *Angew. Chem., Int. Ed. Engl.* **1999**, *38*, 1292. (j) Khan, M. I.; Yohannes, E.; Dödens, R. J.; Tabussum, S.; Cevik, S.; Manno, L.; Powell, D. *Cryst. Eng.* **1999**, *2*, 171. (k) Khan, M. I.; Yohannes, E.; Powell, D. *Inorg. Chem.* **1999**, *38*, 212. (l) Coué, V.; Dessapt, R.; Bujoli-Doeuff, M.; Evain, M.; Jobic, S. *Inorg. Chem.* **2007**, *46*, 2824. (m) Bassil, B. S.; Dickman, M. H.; Kammer, B.; Kortz, U. *Inorg. Chem.* **2007**, *46*, 2452. (n) Kong, X.-J.; Ren, Y.-P.; Zheng, P.-Q.; Long, Y.-X.; Long, L.-S.; Huang, R.-B.; Zheng, L.-S. *Inorg. Chem.* **2006**, *45*, 10702.

(5) (a) Day, V. W.; Klemperer, W. G.; Yagasaki, A. *Chem. Lett.* **1990**, 1267. (b) Day, V. W.; Klemperer, W. G.; Yaghi, O. M. *J. Am. Chem. Soc.* **1989**, *111*, 4518. (c) Day, V. W.; Klemperer, W. G.; Yaghi, O. M. *J. Am. Chem. Soc.* **1989**, *111*, 5959. (d) Hou, D.; Hagen, K. S.; Hill, C. L. *J. Am. Chem. Soc.* **1992**, *114*, 5864. (e) Müller, A.; Penk, M.; Rohlfing, R.; Krickemeyer, E.; Döring, J. *Angew. Chem., Int. Ed. Engl.* **1990**, *29*, 926. (f) Hou, D.; Hagen, K. S.; Hill, C. L. *J. Chem. Soc., Chem. Commun.* **1993**, 426. (g) Chen, Y.; Gu, X.; Peng, J.; Shi, Z.; Yu, H.; Wang, E.; Hu, N. *Inorg. Chem. Commun.* **2004**, *7*, 705. (h) Hayashi, Y.; Fukuyama, K.; Takatera, T.; Uehara, A. *Chem. Lett.* **2000**, *29*, 770. (i) Johnson, G. K.; Schlemper, E. O. *J. Am. Chem. Soc.* **1978**, *100*, 3645. (j) Müller, A.; Penk, M.; Krickemeyer, E.; Bögge, H.; Walberg, H.-J. *Angew. Chem., Int. Ed. Engl.* **1988**, *27*, 1719. (k) Müller, A.; Rohlfing, R.; Döring, J.; Penk, M. *Angew. Chem., Int. Ed. Engl.* **1991**, *30*, 588. (l) Khenkin, A. M.; Weiner, L.; Neumann, R. *J. Am. Chem. Soc.* **2005**, *127*, 9988. (m) Khenkin, A. M.; Neumann, R. *Angew. Chem., Int. Ed. Engl.* **2000**, *39*, 4088. (n) Khenkin, A. M.; Weiner, L.; Wang, Y.; Neumann, R. *J. Am. Chem. Soc.* **2001**, *123*, 8531. (o) Haimov, A.; Neumann, R. *Chem. Commun.* **2002**, 876. (p) Maayan, G.; Ganchegui, B.; Leitner, W.; Neumann, R. *Chem. Commun.* **2006**, 2230. (q) Gaspar, A. R.; Evtuguin, D. V.; Neto, C. P. *Ind. Eng. Chem. Res.* **2004**, *43*, 7754. (r) Bose, A.; He, P.; Liu, C.; Ellman, B. D.; Twieg, R. J.; Huang, S. D. *J. Am. Chem. Soc.* **2002**, *124*, 4.

(6) (a) LaDuca, R. L., Jr.; Rarig, R. S., Jr.; Zubieta, J. *Inorg. Chem.* **2001**, *40*, 607. (b) Hagrman, P. J.; Hagrman, D.; Zubieta, J. *Inorg. Chem.* **2001**, *40*, 2800. (c) Yuan, M.; Li, Y. G.; Wang, E. B.; Lu, Y.; Hu, C. W.; Hu, N. H.; Jia, H. Q. *J. Chem. Soc., Dalton Trans.* **2002**, 2916. (d) Lu, Y.; Wang, E. B.; Yuan, M.; Luan, G. Y.; Li, Y. G. *J. Chem. Soc., Dalton Trans.* **2002**, 3029. (e) Luan, G. Y.; Li, Y. G.; Wang, S. T.; Wang, E. B.; Han, Z. B.; Hu, C. W.; Hu, N. H.; Jia, H. Q. *J. Chem. Soc., Dalton Trans.* **2003**, 233. (f) Lü, J.; Shen, E. H.; Yuan, M.; Li, Y. G.; Wang, E. B.; Hu, C. W.; Xu, L.; Peng, J. *Inorg. Chem.* **2003**, *42*, 6956. (g) Chen, Y.-M.; Wang, E.-B.; Lin, B.-Z.; Wang, S.-T. *J. Chem. Soc., Dalton Trans.* **2003**, 519. (h) Li, Y. G.; Wang, E. B.; Zhang, H.; Luan, G. Y.; Hu, C. W.; Hu, N. H.; Jia, H. Q. *J. Solid State Chem.* **2002**, *163*, 10. (i) Lin, B. Z.; Liu, S. X. *Chem. Commun.* **2002**, 2126. (j) Pan, C. L.; Xu, J. Q.; Li, G. H.; Chu, D. Q.; Wang, T. G. *Eur. J. Inorg. Chem.* **2003**, 1514. (k) Debord, J. R. D.; Haushalter, R. C.; Meyer, L. M.; Rose, D. J.; Zapf, P. J.; Zubieta, J. *Inorg. Chim. Acta* **1997**, *256*, 165.

(7) (a) Müller, A.; Döring, J. *Z. Anorg, Allg. Chem.* **1991**, *595*, 251. (b) Huan, G. H.; Greaney, M. A.; Jacobson, A. J. *Chem. Commun.* **1991**, 260. (c) Müller, A.; Döring, J. *Angew. Chem., Int. Ed. Engl.* **1988**, *27*, 1721. (d) Müller, A.; Döring, J.; Bögge, H. *Chem. Commun.* **1991**, 273. (e) Bu, W. M.; Ye, L.; Yang, G. Y.; Shao, M. C.; Pan, Y. G.; Xu, J. Q. *Chem. Commun.* **2000**, 1279. (f) Dumas, E.; Livage, C.; Halut, S.; Hervé, G. *Chem. Commun.* **1996**, 2437.

(8) (a) Barra, A.-L.; Gatteschi, D.; Pardi, L.; Müller, A.; Döring, J. *J. Am. Chem. Soc.* **1992**, *114*, 8509. (b) Gatteschi, D.; Pardi, L.; Barra, A.-L.; Müller, A.; Döring, J. *Nature* **1991**, *354*, 463.

(9) (a) Zhou, G.; Xu, Y.; Guo, C.; Zheng, X. *Inorg. Chem. Commun.* **2007**, *10*, 849. (b) Zheng, S.-T.; Zhang, J.; Xu, J.-Q.; Yang, G.-Y. *J. Solid State Chem.* **2005**, *178*, 3740. (c) Zheng, S.-T.; Zhang, J.; Yang, G.-Y. *J. Mol. Struct.* **2005**, *752*, 25. (d) Qi, Y.; Li, Y.; Wang, E.; Jin, H.; Zhang, Z.; Wang, X.; Chang, S. *Inorg. Chim. Acta* **2007**, *360*, 1841. (e) Cui, X.-B.; Sun, Y.-Q.; Yang, G.-Y. *Inorg. Chem. Commun.* **2003**, *6*, 259. (f) Zheng, S.-T.; Zhang, J.; Xu, J.-Q.; Yang, G.-Y. *J. Solid State Chem.* **2005**, *178*, 3695. (g) Cui, X.; Xu, J.; Li, Y.; Sun, Y.; Yang, G. *Eur. J. Inorg. Chem.* **2004**, 1051. (h) Zheng, S.-T.; Zhang, J.; Yang, G.-Y. *Inorg. Chem.* **2005**, *44*, 2426.

250−400 °C). We have utilized an organic free linker, aqua−lanthanide complex $[Ln^{III}(H_2O)_n]^{3+}$ to avoid the decomposition of the resulting materials at around 400 °C. We have synthesized three new compounds $[\{Ln(H_2O)_6\}_2As_8V_{14}O_{42}(SO_3)]\cdot 8H_2O$, Ln = La^{3+} (**1**), Sm^{3+} (**2**), and Ce^{3+} (**3**), starting from an ammonium salt of this cluster, $[NH_4]_6[As_8V_{14}O_{42}(SO_3)]$. We have described the synthesis, crystal structures, and spectroscopic and thermal properties of compounds **1**−**3**, including their temperature-dependent magnetic behaviors. To our knowledge, this is the first V/As/O heteropoly-system-based coordination polymer that is free of organic moieties and stable up to 520 °C. Even though the literature on polymeric POMs/POVs (one-dimensional, two-dimensional, or three-dimensional networks), which are connected through rare earth metal ions, d-block transition metal ion/coordination complex cations is abundant,[9−11] there are no reports on polymeric 'V/As/O' type POVs, in which the POV cluster units are linked by a lanthanide ion/lanthanide complex cation. Compounds **1**, **2**, and **3** are such examples of lanthanide-linked POV-based polymeric materials that are also important in terms of magnetism.

Experimental Section

Materials and Methods. The POM compound (as precursor for the present system) $[NH_4]_6[As_8V_{14}O_{42}(SO_3)]$ was synthesized following a procedure described in the literature.[7a] All other chemicals were obtained from a commercial source and used without further purification. Hydrogen and sulfur contents were determined by a FLASH EA series 1112 CHNS analyzer. Infrared spectra of solid samples were obtained as KBr pellets on a JASCO-5300 FT−IR spectrophotometer. Thermogravimetric analyses were carried out on a STA 409 PC analyzer, and corresponding masses were analyzed with a QMS 403 C mass analyzer, under a flow of N_2 gas with a heating rate of 5 °C min^{-1}, in the temperature range 30−1100 °C. Electron spin resonance (ESR) spectra were recorded on a Bruker ECS 106 spectrometer. The reflectance UV−visible spectra were measured using a 3101 Philips spectrophotometer. The solid powders of samples were spread over grease on a glass plate, and the diffuse reflectance spectra obtained were the Kubelka−Munk corrected with grease (on glass plate) background spectra. The powder X-ray diffraction patterns were recorded using Cu Kα (λ = 1.54 Å) radiation on a Phillips PW 3710 diffractometer at a scanning speed of 3° min^{-1}. For compound $[\{La(H_2O)_6\}_2As_8V_{14}O_{42}(SO_3)]\cdot 8H_2O$ (**1**), the variable-temperature (24−294 K) magnetic susceptibility measurements were performed using the Faraday technique with a setup comprising a George Associates Lewis Coil force magnetometer, a CAHN microbalance, and an Air Products cryostat. $Hg[Co(NCS)_4]$ was used as the standard. For compounds $[\{Sm(H_2O)_6\}_2As_8V_{14}O_{42}(SO_3)]\cdot 8H_2O$ (**2**) and $[\{Ce(H_2O)_6\}_2As_8V_{14}O_{42}(SO_3)]\cdot 8H_2O$ (**3**), magnetic studies were performed using crystalline samples on a vibrating sample magnetometer in a physical property measurement system (PPMS, Quantum Design, USA). Diamagnetic corrections (-481.85×10^{-6} cgsu for compounds **1**, **2**, and **3**; all three compounds have same number of oxygen, arsenic, and sulfur atoms), calculated from Pascal's constants, were used to obtain the respective molar paramagnetic susceptibilities. Inductively coupled plasma (ICP) analyses were carried out on a JY ULTIMA spectrometer.

A General Synthetic Procedure for Compounds 1−3. The starting precursor $[NH_4]_6[As_8V_{14}O_{42}(SO_3)]$ (0.30 g, 0.14 mmol) was dissolved in 5 mL of H_2O taken in one branch of a U-shaped tube. The other branch of the U tube was filled with 5 mL of H_2O, in which 0.92 mmol of $Ln(NO_3)_3\cdot 6H_2O$ ($[La(NO_3)_3\cdot 6H_2O$, 0.40 g; $Sm(NO_3)_3\cdot 6H_2O$, 0.41 g; $Ce(NO_3)_3\cdot 6H_2O$, 0.40 g) was dissolved. The two branches of U-shaped tube were separated by a G4 crucible bead. After one week, single crystals (**1**−**3**) were separated out and washed thoroughly with water, and one of the single crystals from each, suitable for X-ray diffraction study, was selected and characterized structurally. The purity of the bulk crystals was checked by X-ray powder diffraction methods.

$[\{La(H_2O)_6\}_2As_8V_{14}O_{42}(SO_3)]\cdot 8H_2O$ (1). Yield: 0.12 g (32% based on ammonium salt of vanadium cluster, the starting precursor). Anal. calcd for $As_8V_{14}SLa_2H_{40}O_{65}$: H, 1.49; S, 1.18; V, 26.39; As, 22.18; La, 10.28. Found: H, 1.47; S, 1.19; V, 26.32 (ICP); As, 22.07 (ICP); La, 9.98 (ICP). Selected data for **1**, FT-IR (cm^{-1}): υ(O−H) 3395 (w); (H−O−H bending) 1620; (V═O) 984, 941; (SO_3^{2-}) 902 (m); (As−O) 687 (m).

$[\{Sm(H_2O)_6\}_2As_8V_{14}O_{42}(SO_3)]\cdot 8H_2O$ (2). Yield: 0.10 g (27% based on ammonium salt of vanadium cluster, the starting precursor). Anal. calcd for $As_8V_{14}SSm_2H_{40}O_{65}$: H, 1.48; S, 1.17; V, 26.16; As, 21.99; Sm, 11.03. Found: H, 1.42; S, 1.29; V, 25.89 (ICP);

(10) (a) Jin, H.; Qin, C.; Li, Y.-G.; Wang, E.-B. *Inorg. Chem. Commun.* **2006**, *9*, 482. (b) Wang, J.-P.; Du, X.-D.; Niu, J.-Y. *J. Solid State Chem.* **2006**, *179*, 3260. (c) Wu, C.-D.; Lu, C.-Z.; Zhuang, H.-H.; Huang, J.-S. *Inorg. Chem.* **2002**, *41*, 5636. (d) Yang, W.; Lu, C.; Zhuang, H. *J. Chem. Soc., Dalton Trans.* **2002**, 2879. (e) Xu, Y.; Nie, L.-B.; Zhu, D.; Song, Y.; Zhou, G.-P.; You, W.-S. *Cryst. Growth Des.* **2007**, *7*, 925. (f) Soghomonian, V.; Chen, Q.; Haushalter, R. C.; Zubieta, J.; O'Connor, C. J. *Science* **1993**, *259*, 1596. (g) Hagrman, D.; Hagrman, P. J.; Zubieta, J. *Angew. Chem., Int. Ed. Engl.* **1999**, *38*, 3165. (h) Hagrman, P. J.; Zubieta, J. *Inorg. Chem.* **2000**, *39*, 3252. (i) Hagrman, D.; Sangregorio, C.; O'Connor, C. J.; Zubieta, J. *J. Chem. Soc., Dalton Trans.* **1998**, 3707. (j) Hagrman, P. J.; Hagrman, D.; Zubieta, J. *Angew. Chem., Int. Ed. Engl.* **1999**, *38*, 2638. (k) Khan, M. I. *J. Solid State Chem.* **2000**, *152*, 105. (l) Khan, M. I.; Yohannes, E.; Powell, D. *Chem. Commun.* **1999**, 23. (m) Khan, M. I.; Yohannes, E.; Dödens, D. *Angew. Chem., Int. Ed. Engl.* **1999**, *38*, 1292. (n) Khan, M. I.; Yohannes, E.; Dödens, R. J.; Tabussum, S.; Cevik, S.; Manno, L.; Powell, D. *Cryst. Eng.* **1999**, *2*, 171. (o) Khan, M. I.; Yohannes, E.; Powell, D. *Inorg. Chem.* **1999**, *38*, 212. (p) Cao, Y.; Zhang, H.; Huang, C.; Yang, Q.; Chen, Y.; Sun, R.; Zhang, F.; Guo, W. *J. Solid State Chem.* **2005**, *178*, 3563. (q) Li, M.-X.; Du, J.; Wang, J.-P.; Niu, J.-Y. *Inorg. Chem. Commun.* **2007**, *10*, 1391. (r) Yi, Z.-H.; Cui, X.-B.; Zhang, X.; Chen, Y.; Xu, J.-Q.; Yang, G.-D.; Liu, Y.-B.; Yu, X.-Y.; Yu, H.-H.; Duan, W.-J. *Inorg. Chem. Commun.* **2007**, *10*, 1448. (s) Lin, B.-Z.; Chen, Y.-M.; Liu, P.-D. *J. Chem. Soc., Dalton Trans.* **2003**, 2474. (t) Liu, C.-M.; Zhng, D.-Q.; Xiong, M.; Zhu, D.-B. *Chem. Commun.* **2002**, 1416. (u) Pan, C.-L.; Xu, J.-Q.; Li, G.-H.; Cui, X.-B.; Ye, L.; Yang, G.-D. *J. Chem. Soc., Dalton Trans.* **2003**, 517. (v) Liu, A.-H.; Wang, S.-L. *Inorg. Chem.* **1998**, *37*, 3415. (w) Sha, J.; Peng, J.; Li, Y.; Zhang, P.; Pang, H. *Inorg. Chem. Commun.* **2008**, *11*, 907. (x) Finn, R. C.; Burkholder, E.; Zubieta, J. *Chem. Commun.* **2001**, 1852. (y) Chen, J.; Sha, J.-Q.; Peng, J.; Shi, Z.-Y.; Dong, B.-X.; Tian, A.-X. *J. Mol. Struct.* **2007**, *846*, 128.

(11) (a) An, H.; Xu, T.; Wang, E.; Meng, C. *Inorg. Chem. Commun.* **2007**, *10*, 1453. (b) Zhang, C.-J.; Chen, Y.-G.; Pang, H.-J.; Shi, D.-M.; Hu, M.-X.; Li, J. *Inorg. Chem. Commun.* **2008**, *11*, 765. (c) Sadakane, M.; Dickman, M. H.; Pope, M. T. *Angew. Chem., Int. Ed. Engl.* **2000**, *39*, 2914. (d) Zhang, Z.; Li, Y.; Chen, W.; Wang, E.; Wang, X. *Inorg. Chem. Commun.* **2008**, *11*, 879. (e) Gan, X.; Zhang, Z.; Yao, S.; Chen, W.; Wang, E.; Zhang, H. *J. Cluster Sci.* **2008**, *19*, 401. (f) Niu, J.-Y.; Wu, Q.; Wang, J.-P. *J. Chem. Soc., Dalton Trans.* **2002**, 2512. (g) Zheng, L.-M.; Wang, Y.; Wang, X.; Korp, J. D.; Jacobson, A. J. *Inorg. Chem.* **2001**, *40*, 1380. (h) Wang, J.-P.; Zhao, J.-W.; Duan, X.-Y.; Niu, J.-Y. *Cryst. Growth Des.* **2006**, *6* (2), 507. (i) Zhang, C.-J.; Chen, Y.-G.; Pang, H.-J.; Shi, D.-M.; Hu, M.-X.; Li, J. *Inorg. Chem. Commun.* **2008**, *11*, 765. (j) Shivaiah, V.; Narashimha Reddy, P. V.; Cronin, L.; Das, S. K. *J. Chem. Soc., Dalton Trans.* **2002**, 3781. (k) Shivaiah, V.; Nagaraju, M.; Das, S. K. *Inorg. Chem.* **2003**, *42*, 6604. (l) Liu, G.; Wei, Y.-G.; Yu, Q.; Liu, Q.; Zhang, S.-W. *Inorg. Chem. Commun.* **1999**, *2*, 434. (m) Yamase, T.; Naruke, H. *J. Chem. Soc., Dalton Trans.* **1991**, 285. (n) Gimbnéz-Saiz, C.; Galán-Mascarós, J. R.; Triki, S.; Coronado, E.; Ouahab, L. *Inorg. Chem.* **1995**, *34*, 524. (o) Zhang, Z.; Qi, Y.; Wang, E.; Li, Y.; Tan, H. *Inorg. Chim. Acta* **2008**, *361*, 1797. (p) An, H.; Wang, E.; Li, Y.; Zhang, Z.; Xu, Lin *Inorg. Chem. Commun.* **2007**, *10*, 299.

Table 1. Crystal Data and Structural Refinement for Compounds **1**−**3**

	1	**2**	**3**
empirical formula	$As_8V_{14}La_2O_{65}SH_{40}$	$As_8V_{14}Sm_2O_{65}SH_{40}$	$As_8V_{14}Ce_2O_{65}SH_{40}$
fw	2702.71	2725.61	2705.13
temp (K)	100	100	293
λ (Å)	0.71073	0.71073	0.71073
crystal system	monoclinic	monoclinic	monoclinic
space group	*P*2(1)/*n*	*P*2(1)/*n*	*P*2(1)/*n*
a (Å)	13.4839(7)	13.4156(3)	13.4934(3)
b (Å)	12.3388(6)	12.2588(3)	12.3983(3)
c (Å)	18.3572(10)	18.2501(4)	18.3992(4)
α (deg)	90.0000	90.000	90.000
β (deg)	108.2570(10)	108.049(3)	108.025(3)
γ (deg)	90.0000	90.000	90.000
V (Å^3)	2900.4(3)	2853.8(10)	2927.0(10)
Z	2	2	2
d_{calcd} (mg m^{-3})	3.049	3.125	3.024
μ (mm^{-1})	8.275	8.971	8.295
F(000)	2472	2692	2476
crystal size (mm^3)	0.22 × 0.18 × 0.10	0.18 × 0.08 × 0.06	0.33 × 0.10 × 0.05
θ range for data collection (deg)	1.65−25.00	1.66−25.00	1.65−25.00
reflns collected/unique	27141/5106	26836/5031	27323 /5147
R (int)	0.0274	0.0293	0.0344
Refinement Method		Full-Matrix Least-Squares on F^2	
data/restraints/params	5106/0/428	5031/0/424	5147/0/424
goodness-of-fit on F^2	1.074	1.065	1.106
R_1/wR_2 [$I > 2\sigma(I)$]	0.0340/0.0914	0.0317/0.0832	0.0439/0.1107
R_1/wR_2 (all data)	0.0386/0.0943	0.0364/0.0867	0.0468/0.1128
largest diff. peak/hole (e Å^{-3})	2.549/−1.011	2.355/−1.067	2.728/−0.701

As, 22.17 (ICP); Sm, 10.88 (ICP). Selected data for **2**, FT-IR (cm^{-1}): (O−H) 3383 (w); (H−O−H bending) 1618; (V═O) 978, 945; (SO_3^{2-}) 904(m); (As−O) 686 (m).

[{Ce(H$_2$O)$_6$}$_2$As$_8$V$_{14}$O$_{42}$(SO$_3$)]·8H$_2$O (3). Yield: 0.12 g (32% based on ammonium salt of vanadium cluster, the starting precursor). Anal. calcd for $As_8V_{14}SCe_2H_{40}O_{65}$: H, 1.49; S, 1.19; V, 26.36; As, 22.16; Ce, 10.36. Found: H, 1.45; S, 1.18; V, 26.55 (ICP); As, 22.38 (ICP); Ce, 10.02 (ICP). Selected data for **3**, FT-IR (cm^{-1}): (O−H) 3400 (w); (H−O−H bending) 1618; (V═O) 979, 941; (SO_3^{2-}) 904 (m); (As−O) 688 (m).

X-Ray Data Collection and Structure Determination. Data were measured at 293(2) K on a Bruker SMART APEX CCD area detector system [λ(Mo Kα) = 0.71073 Å], with a graphite monochromator; 2400 frames recorded with an ω scan width of 0.3°, each for 5 s; a crystal detector distance of 60 mm; and a collimator of 0.5 mm. The data were reduced using SAINTPLUS,[12] and the structures were solved using SHELXS-97[13] and refined using SHELXL-97.[14] All non-hydrogen atoms were refined anisotropically. We tried to locate the hydrogen atom of solvent water molecules through differential Fourier maps but could not succeed. A summary of the crystallographic data and structure determination parameters for **1**−**3** is provided in Table 1. Selected bond lengths and angles for compound **1** are provided in Table 2 (see the Supporting Information for bond lengths and angles for compounds **2** and **3**).

Table 2. Selected Bond Lengths [Å] and Angles [deg] for Compound **1**

V(1)−O(1)	1.637(4)	V(1)−O(4)	1.952(4)
V(2)−O(5)	1.612(4)	V(3)−O(7)	1.602(4)
V(3)−O(6)	1.967(4)	V(4)−O(10)	1.616(4)
V(4)−O(9)	1.943(4)	V(5)−O(13)	1.604(4)
V(6)−O(14)	1.987(4)	V(7)−O(17)	1.611(4)
As(1)−O(15)	1.756(4)	As(1)−O(21)	1.782(4)
La(1)−O(28)	2.508(5)	La(1)−O(27)	2.527(5)
O(22)−S(1)	1.389(11)	O(23)−S(1)	1.463(10)
O(1)−V(1)−O(4)	109.9(2)	O(5)−V(2)−O(3)	107.7(2)
O(5)−V(2)−O(2)	106.26(19)	O(7)−V(3)−O(6)	103.69(19)
O(10)−V(4)−O(9)	106.83(19)	O(13)−V(5)−O(15)	96.5(2)
O(15)−V(5)−O(14)	79.39(17)	O(16)−V(6)−O(4)	104.9(2)
O(11)−As(3)−O(19)	99.77(19)	O(18)−As(4)−O(14)	96.6(2)
O(18)−As(4)−O(19)	99.95(19)	O(1)−La(1)−O(28)	138.20(16)
O(1)−La(1)−O(27)	141.85(17)	O(28)−La(1)−O(27)	77.20(18)
O(1)−La(1)−O(26)	74.57(16)	O(28)−La(1)−O(26)	133.16(16)
As(1)−O(6)−V(2)	122.0(2)	As(2)−O(8)−V(3)	136.6(2)
As(3)−O(11)−V(4)	123.7(2)	As(2)−O(12)−V(5)	132.9(2)
O(23)−O(22)−S(1)	73.8(9)	O(22)−O(23)−S(1)	65.7(8)
S(1)−O(23)−O(24)	60.0(5)	O(22)−O(23)−V(5)	79.7(8)
O(22)−S(1)−O(23)	40.5(5)	O(22)−S(1)−O(24)	106.7(7)

Results and Discussion

Synthesis and Characterization. The majority of the POM/POV-supported metal complexes with multi-dimensional structures, reported earlier, have been synthesized by hydrothermal techniques.[10] Some POM/POV polymeric materials are reported to be synthesized under ambient conditions.[11] We have isolated compounds [{La(H$_2$O)$_6$}$_2$As$_8$V$_{14}$O$_{42}$(SO$_3$)]·8H$_2$O (**1**), [{Sm(H$_2$O)$_6$}$_2$As$_8$V$_{14}$O$_{42}$(SO$_3$)]·8H$_2$O (**2**), and [{Ce(H$_2$O)$_6$}$_2$As$_8$V$_{14}$O$_{42}$(SO$_3$)]·8H$_2$O (**3**) in a unique wet synthesis at room temperature. We have introduced a new technique (a controlled synthesis), called "U-tube synthesis" to isolate the crystalline products of compounds **1**−**3**. Even though the reaction (eq 1, where Ln = La^{3+} (**1**), Sm^{3+} (**2**), and Ce^{3+} (**3**)) to obtain these compounds looks simple, the mixing of both reactants in an aqueous medium invariably results in the immediate formation of a brown precipitate, which could not be characterized by single-crystal X-ray structure determination techniques. We, thus, performed the synthesis using a slow mixing technique called "U-tube synthesis". The schematic representation of this technique is shown in Scheme 1.

(12) *SAINT*; Bruker Analytical X-ray Systems, Inc.: Madison, WI, 1998.
(13) Sheldrick, G. M. *SHELXS-97*; University of Göttingen: Göttingen, Germany, 1997.
(14) Sheldrick, G. M. *SHELXL-97*; University of Göttingen: Göttingen, Germany, 1997.

$$H_2O[NH_4]_6[As_8V_{14}O_{42}(SO_3)] + 2Ln(NO_3)_3 \rightarrow [\{Ln(H_2O)_6\}_2As_8V_{14}O_{42}(SO_3)] + 6NH_4NO_3 \quad (1)$$

The two branches of the U-shaped tube were separated by a G4 crucible bead. The dissolved reactant components in water were taken into the two branches of the U tube (as shown in Scheme 1) to mix slowly, and single crystals, suitable for X-ray structure determination, were formed on the side wall of the U tube. These crystals were collected and washed with cold water.

Description of the Crystal Structures. The basic building block for the compounds **1**−**3** is $[As_8V_{14}O_{42}(SO_3)]^{6-}$. The asymmetrical unit contains seven vanadium atoms, four arsenic atoms, half of a disordered SO_3^{2-} molecule (with half-occupancy of both sulfur and oxygen atoms), a $[Ln(H_2O)_6]^{3+}$ ion attached to the cluster anion by a coordinate covalent bond, and four crystal water molecules. Thus, the general formula for these compounds is described as $[\{Ln(H_2O)_6\}_2As_8V_{14}O_{42}(SO_3)]\cdot 8H_2O$. The thermal ellipsoidal plot of the asymmetric unit of the lanthanum analogue is shown in Figure 1. The molecular structure of compound **1** is shown in Figure 2. The cluster anion $[As_8V_{14}O_{42}(SO_3)]^{6-}$ consists of 14 distorted $\{VO_5\}$ square pyramids and eight $\{AsO_3\}$ triangular groups, with a disordered SO_3^{2-} anion at the center of the cluster anion, resulting in the overall charge of the sulfite encapsulated cluster being −6. A handlelike $\{As_2O_5\}$ moiety is formed from two $\{AsO_3\}$ triangular groups that are linked together by an oxygen bridge. The 14 $\{VO_5\}$ square pyramids, which are connected by edge sharing, are further linked to $\{As_2O_5\}$ units by sharing oxygen atoms, resulting in a spherelike structure with an approximate D_{2d} symmetry. This cluster anion can also be described by the formation of an octagon-like eight-membered ring, formed by the edge-shared fusion of eight $\{VO_5\}$ square pyramids and two sets of three vanadium ions which attach diametrically opposed centers on the octagons, as shown in Scheme 2. In compounds **1**−**3**, all of the $\{VO_5\}$ square pyramids on respective $\{V_{14}\}$ clusters have typical geometries with apical V═O terminal bond distances and basal V−O (in which oxygen is bridging type) bond distances of 1.598(5)−1.641(5) and 1.918(4)−1.998(4) Å, respectively. In the $\{As_2O_5\}$ fragments, the As−O distances are in the range of 1.753(4)−1.797(5) Å with As−O−As angles in the range of 135.3(2)−136.6(2)°.

In the structures of **1**−**3**, each $\{V_{14}\}$ cluster is coordinated to its six surrounding lanthanide ions (Ln^{3+}) through terminal oxygen atoms of the $\{V_{14}\}$ cluster, as shown in Figure 3a. Similarly, each Ln^{3+} (where Ln^{3+} = La^{3+}, Sm^{3+}, and Ce^{3+})

Scheme 1

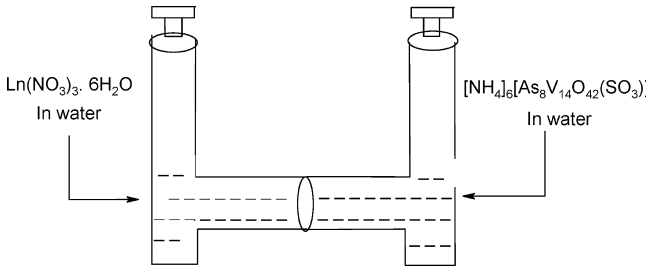

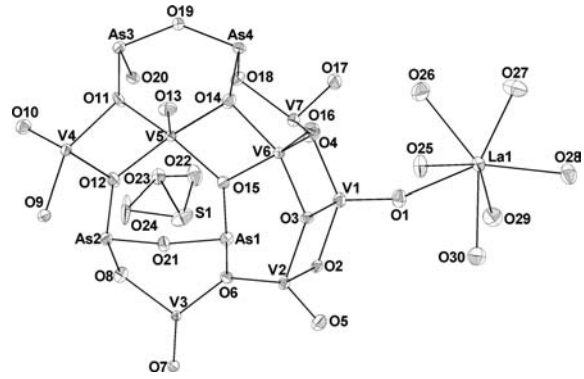

Figure 1. The thermal ellipsoidal plot (50% probability) of the asymmetric unit of compound $[\{La(H_2O)_6\}_2As_8V_{14}O_{42}(SO_3)]\cdot 8H_2O$ (**1**) excluding lattice water molecules.

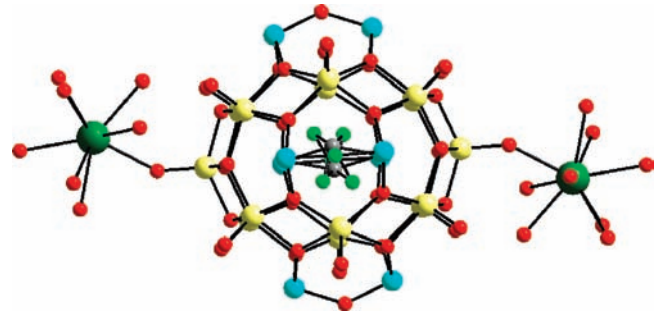

Figure 2. The molecular structure of $[\{La(H_2O)_6\}_2As_8V_{14}O_{42}(SO_3)]$ in compound **1**. Color code: La, dark green; V, yellow; As, cyan; O, red; S, medium gray; O-coordinated sulfur, light green.

Scheme 2

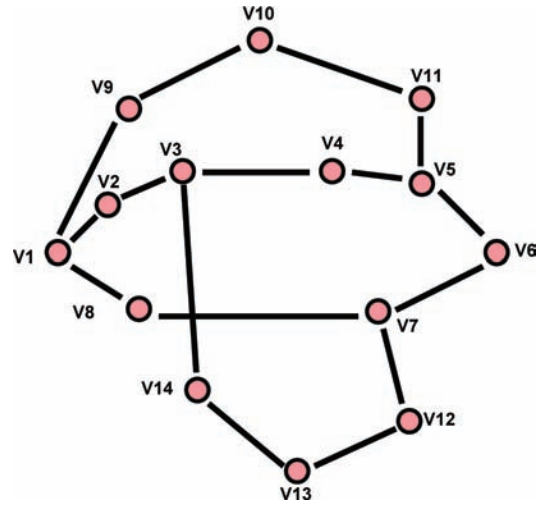

ion is coordinated to three $\{V_{14}\}$ cluster anions (Figure 3b); the remaining coordination sites of the lanthanide ions are filled by six water molecules with bond lengths (for La^{3+} analogue) in the range of 2.500(4)−2.683(4) Å. Thus, in the crystal structure, each La^{3+} ion (that has a coordination number of nine) attains monocapped square-antiprism geometry. The coordination of lanthanum ions to the $\{V_{14}\}$ cluster anions extends throughout the crystal and results in a new type of two-dimensional (2D) network, as shown in Figure 4. The construction of this 2D network can also be described as the formation of a chainlike arrangement (Figure 5), in which adjacent $\{V_{14}\}$ clusters are linked by two aqua−lanthanum complexes, and then these chains are

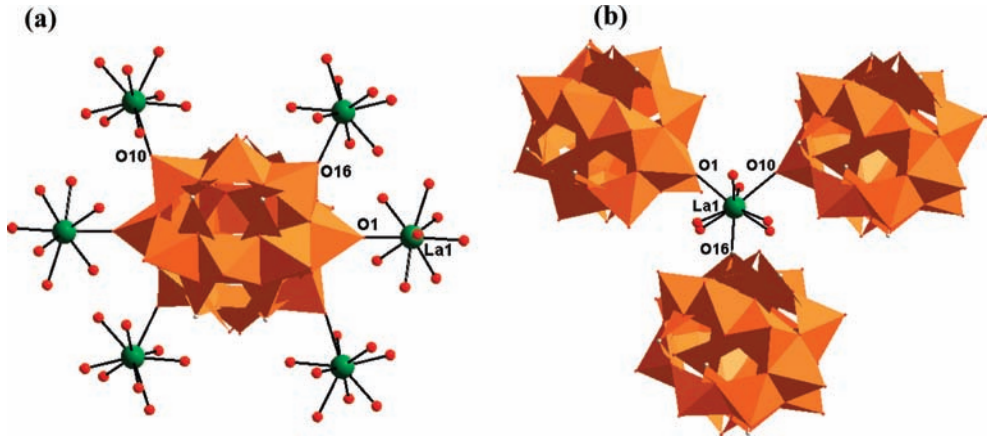

Figure 3. (a) The coordination environment of a POV cluster anion, $[As_8V_{14}O_{42}(SO_3)]^{6-}$, with its surrounding lanthanum−aqua complex cations in compound **1**. (b) The coordination environment of a lanthanum cation with its surrounding POM clusters i in compound **1**. Color code: O, red, La, dark green. Polyhedra are shown in golden yellow color.

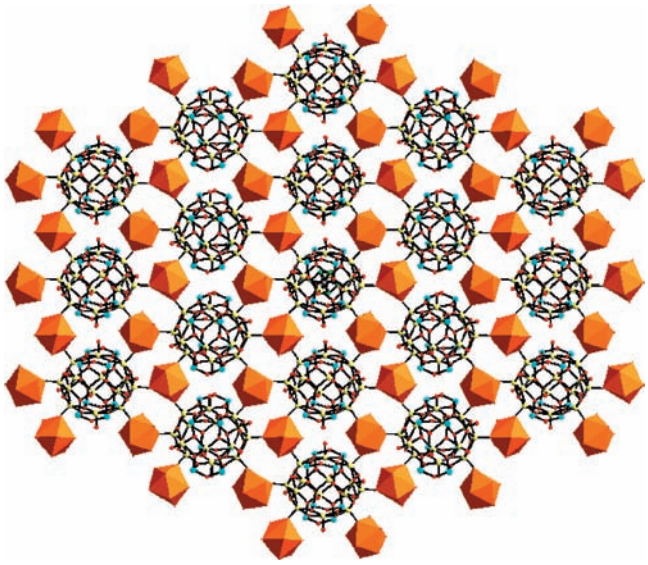

Figure 4. The two-dimensional (2D) layered structure of $[\{La(H_2O)_6\}_2As_8V_{14}O_{42}(SO_3)]$ in compound **1**. Cluster anions are shown in ball-and-stick model representation, and the lanthanum-aqua complexes are shown in polyhedral representation. Color code: O, red; V, yellow; As, cyan; S, medium gray; O from SO_3 molecule, light green. Polyhedra are shown in golden yellow color.

laterally interlinked by Ln−O−V bonds (each of these bonds uses V=O terminal bonds), leading to a 2D polymeric layered structure of $[\{Ln(H_2O)_6\}_2As_8V_{14}O_{42}(SO_3)]_n$ (Figure 4). As shown in the network (Figures 3a and 4), each $\{V_{14}\}$ cluster anion $\{As_8V_{14}O_{42}(SO_3)\}^{6-}$ acts as hexadentate ligand and, hence, coordinates six surrounding lanthanum complex ions. Generally, a higher coordination number for a POM anion, coordinating a metal complex ion, is very rarely known. A Silverton-type POM cluster anion has been shown to have a coordination number of 9 in a three-dimensional network (which was synthesized hydrothermally) consisting of $[GdMo_{12}O_{42}]^{9-}$ and $[Gd(H_2O)_3]^{3+}$ as anions and cations, respectively.[15] For a POV cluster anion coordinating a metal complex ion, a higher coordination number is observed for a lanthanide-capped POV anion.[16] In all of the compounds **1**−**3**, the encapsulated sulfite anion SO_3^{2-} is disordered over two positions, and these positions are related by symmetry operations (Figure 6).

In compounds **1**−**3**, the overall oxygen bonding modes can be divided into five categories, for example, for lanthanum analogue $[\{La(H_2O)_6\}_2As_8V_{14}O_{42}(SO_3)]\cdot 8H_2O$ (**1**), (i) V=O_t (O_t = terminal oxygen) bond lengths observed in the range of 1.602(4)−1.637(4) Å, (ii) μ_3-bridging oxygen lengths in the range of 1.756(4)−1.994(4) Å, (iii) μ_2-bridging oxygen bond lengths in the range of 1.771(4)−1.783(4) Å, (iv) in SO_3^{2-} molecule, S−O bond lengths in the range of 1.389(11)−1.623(10) Å, and (v) La−O bond lengths in the range of 2.500(4)−2.683(4) Å. Two-dimensional polymeric structures based on two types of POV units ($[MV_{13}O_{38}]^{7-}$ and $[MV_{12}O_{38}]^{12-}$, M = Mn, Ni) are described in the recent literature.[16]

Identification of Water Clusters. Compounds **1**−**3** were isolated from the aqueous medium, and expectedly they contain lattice water molecules. It is notable that all of the coordinated ligands are water molecules, because we avoided organic ligands to achieve an organic free material. So, it is not surprising that noncovalent hydrogen-bonding interactions of the type O−H···O would be observed. We have analyzed these supramolecular interactions in detail for compound **1**, and we observed a "Z"-shaped water hexamer $(H_2O)_6$, which is formed exclusively from lattice water molecules O31, O32, and O33 and their symmetry equivalent atoms, as shown in Figure 7a. This water hexamer, in turn, is hydrogen-bonded with eight surrounding lanthanum-coordinated water molecules (O25, O26, O27, and O30 and their symmetry equivalent atoms), furnishing a $(H_2O)_{14}$ cluster, which is further hydrogen-bonded to two lattice water molecules (O34 and its symmetry equivalent atom), resulting in a $(H_2O)_{16}$ cluster, as shown in Figure 7b. The hydrogen atoms of lanthanum coordinated and lattice water molecules could not be located in the crystal structures, and thus the hydrogen-bonding distances of this water structure are taken as O···O distances (see Table S4 in Supporting Information).

(15) Wu, C.-D.; Lu, C.-Z.; Zhuang, H.-H.; Huang, J.-S. *J. Am. Chem. Soc.* **2002**, *124*, 3836.

(16) Liu, S.; Li, D.; Xie, L.; Cheng, H.; Zhao, X.; Su, Z. *Inorg. Chem.* **2006**, *45*, 8036.

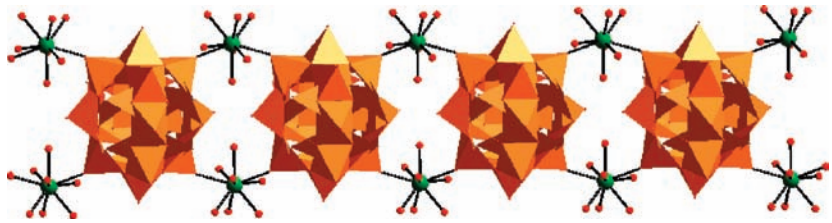

Figure 5. Two adjacent $\{V_{14}\}$ clusters linked by two lanthanum-aqua complexes leading to a one-dimensional (1D) chain. Cluster anions are shown in polyhedral representation, and lanthanum-aqua complexes are represented in ball-and-stick model represenation. Color code: O, red; La, dark green. Polyhedra are shown in golden yellow color.

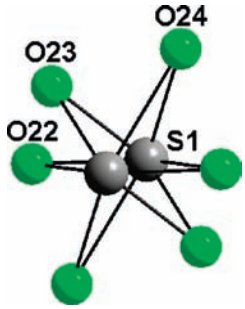

Figure 6. A disordered SO_3^{2-} molecule, which is encapsulated in the cavity of the $[As_8V_{14}O_{42}]^{4-}$ cluster anion, is represented in ball-and-stick model representation. Color code: O, light green; S, medium gray. The cluster anion is not shown here.

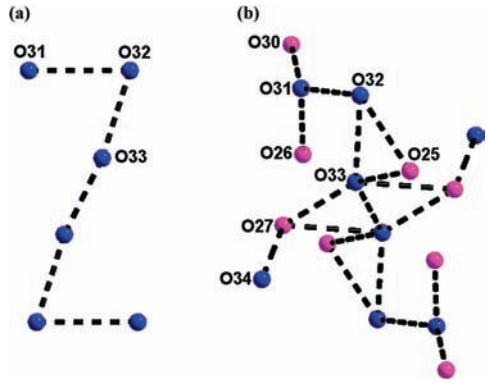

Figure 7. (a) A "Z"-shaped water hexamer $(H_2O)_6$, which is formed exclusively from lattice water molecules O31, O32, and O33, and their symmetry-equivalent atoms. (b) The hydrogen bonding interactions of this water hexamer with its surrounding eight lanthanum-coordinated water molecules (O25, O26, O27, and O30 and their symmetry-equivalent atoms) furnishing a $(H_2O)_{14}$ cluster, which is further hydrogen-bonded to two lattice water molecules (O34 and its symmetry-equivalent atom), resulting finally in a $(H_2O)_{16}$ cluster. Color code: lattice water molecules, blue; lanthanum-coordinated water molecules, purple. Black dotted lines represent the hydrogen-bonding interactions.

Interestingly, the O33 of the water hexamer undergoes bifurcating hydrogen-bonding interactions with O25 and O27 of the lanthanum complex. Similarly, the O31 water oxygen is hydrogen-bonded to O26 and O30 water molecules in a bifurcating fashion. The resulting water cluster $(H_2O)_{16}$ is further hydrogen-bonded to its six surrounding $\{V_{14}\}$ clusters that use both terminal and bridging oxygen atoms of the cluster anions, resulting in an intricate three-dimensional supramolecular network, as shown in Figure 8. Similarly, in the crystal structure, each $\{V_{14}\}$ cluster is hydrogen-bonded with six $(H_2O)_{16}$ water clusters around it (Figure 9).

Single-crystal X-ray diffraction analysis revealed that compounds **1**−**3** are isostructural, and thereby the unit cell dimensions, volumes, and other related data for structure determinations vary only slightly (Table 1). Bond valence sum (BVS) calculations,[17] of compounds **1**−**3**, suggest that all vanadium and arsenic atoms exist in the +4 and +3 oxidation state, respectively (BVS details are presented in the Supporting Information, section S6).

Spectroscopy. The diffuse reflectance spectra of compounds **1**−**3** and the ammonium salt of $\{V_{14}\}$, recorded at room temperature, are presented in Figure 10. All compounds show a broad feature in the region of 700−1100 nm, and two more additional peaks in the region of 200−360 nm. The broad peaks around 1100 nm are assigned to d−d transitions for the $V^{4+}(d^1)$ ion. The sharp band around 350 nm is due to the ligand-to-metal charge transfer (O → V) transition. Similar transitions are observed in the electronic spectra for other related compounds.[18] A weak feature is clearly observed around 800 nm in the electronic spectrum of compound $[\{Sm(H_2O)_6\}_2As_8V_{14}O_{42}(SO_3)]\cdot 8H_2O$ (**2**) (see the inset of Figure 10), which can be assigned to the f−f transition of the Sm^{3+} ion.

The ESR spectra for compounds **1**−**3** were recorded at 170 K and are shown in the Supporting Information (section S2). The single-line ESR signals (except the spectrum of compound **2**) at $g = 1.967$ for **1**, $g = 1.967$ for **2**, and $g = 1.970$ for **3** confirm that the vanadium atoms, present in compounds **1**−**3**, are in +4 oxidation states. In the case of compound **2**, an additional feature is observed at $g = 5.924$, due to the presence of the Sm^{3+} ion. The powder X-ray diffraction studies of compounds **1**−**3**, confirming that these are isostructural compounds, are shown in section S3 in the Supporting Information.

Magnetism. The variable-temperature magnetic susceptibility of compounds $[\{Sm(H_2O)_6\}_2As_8V_{14}O_{42}(SO_3)]\cdot 8H_2O$ (**2**) and $[\{Ce(H_2O)_6\}_2As_8V_{14}O_{42}(SO_3)]\cdot 8H_2O$ (**3**) was measured between 2 and 300 K. Figure 11a and b show the magnetic behaviors of compounds **2** and **3** in the form of χ_M versus T and product $\chi_M T$ versus T plots, respectively. The $\chi_M T$ values of compounds **2** and **3** at 300 K are 3.76 cm^3 K mol^{-1} (5.49 μ_B) and 4.35 cm^3 K mol^{-1} (5.90 μ_B), respectively, which are considerably smaller than those expected for the total spin-only value 5.25 cm^3 K mol^{-1} (6.48 μ_B), which corresponds to the presence of 14 noninteracting V^{4+} ions with $S = 1/2$ in the $\{V_{14}\}$ cluster anion. However, these room temperature values (3.76 cm^3 K mol^{-1} for compound **2** and 4.35 cm^3 K mol^{-1} for compound **3**) are relatively higher than the room temperature $\chi_M T$ value (2.48 cm^3 K mol^{-1}; 4.45 μ_B) of the discrete

(17) Brown, I. D.; Altermatt, D. *Acta Crystallogr.* **1985**, *B41*, 244.
(18) Yuan, M.; Li, Y.; Wang, E.; Tian, C.; Wang, L.; Hu, C.; Hu, N.; Jia, H. *Inorg. Chem.* **2003**, *42*, 3670.

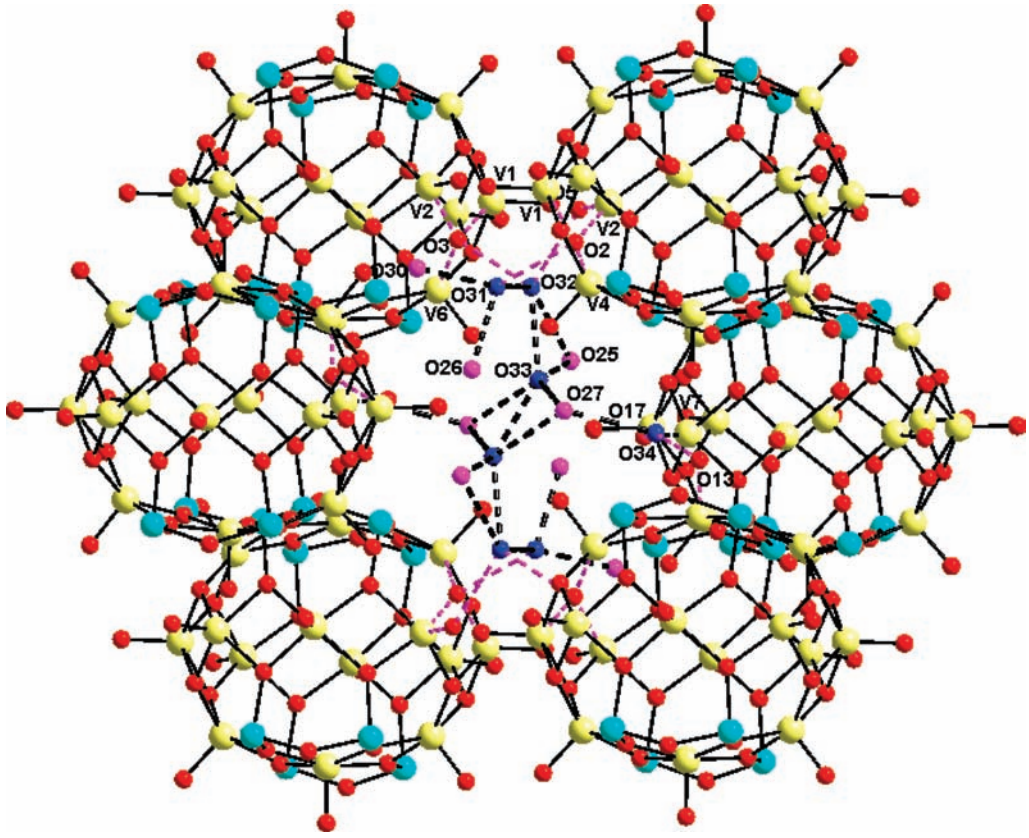

Figure 8. The hydrogen bonding situation around a $(H_2O)_{16}$, showing its interactions with six surrounding cluster anions, $[As_8V_{14}O_{42}(SO_3)]^{6-}$. Color code: lattice water molecules, blue; lanthanum-coordinated water molecules, purple; V, yellow; As, cyan; O, red. Black dotted lines represent the hydrogen-bonding interactions.

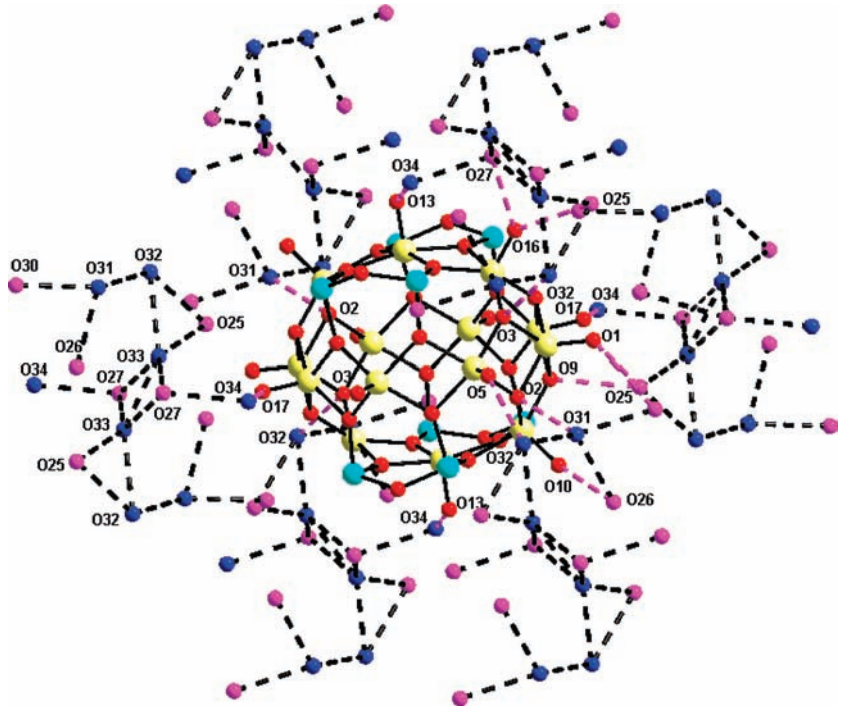

Figure 9. Supramolecular hydrogen-bonding interaction around the cluster anion, $[As_8V_{14}O_{42}(SO_3)]^{6-}$, which interacts with six surrounding $(H_2O)_{16}$ clusters. Color codes are the same as in the caption of Figure 8.

compound $[NH_4]_6[As_8V_{14}O_{42}(SO_3)]$.[8a] This obviously indicates that the Sm^{3+} ion ($4f^5$, $S = 5/2$) and Ce^{3+} ion ($4f^1$, $S = 1/2$) linkers contribute to the overall magnetic susceptibilities of compounds **2** and **3**, respectively, at room temperature. There are two lanthanide ions per POV cluster anion $[As_8V_{14}O_{42}(SO_3)]^{6-}$ in these compounds.

Sm^{3+} has a larger experimental value of μ_{obsd} (1.5−1.6 μ_B) compared to its expected/theoretical value of μ_J (0.85

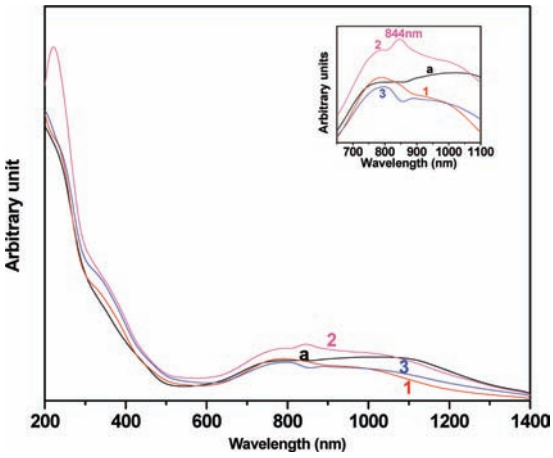

Figure 10. Diffuse reflectance electronic spectra of $[NH_4]_6[As_8V_{14}O_{42}(SO_3)]$ (black line), compound **1** (red line), compound **2** (purple line), and compound **3** (blue line). The inset picture is the enlarged view, to show the weak feature of Sm^{3+} in compound **2**.

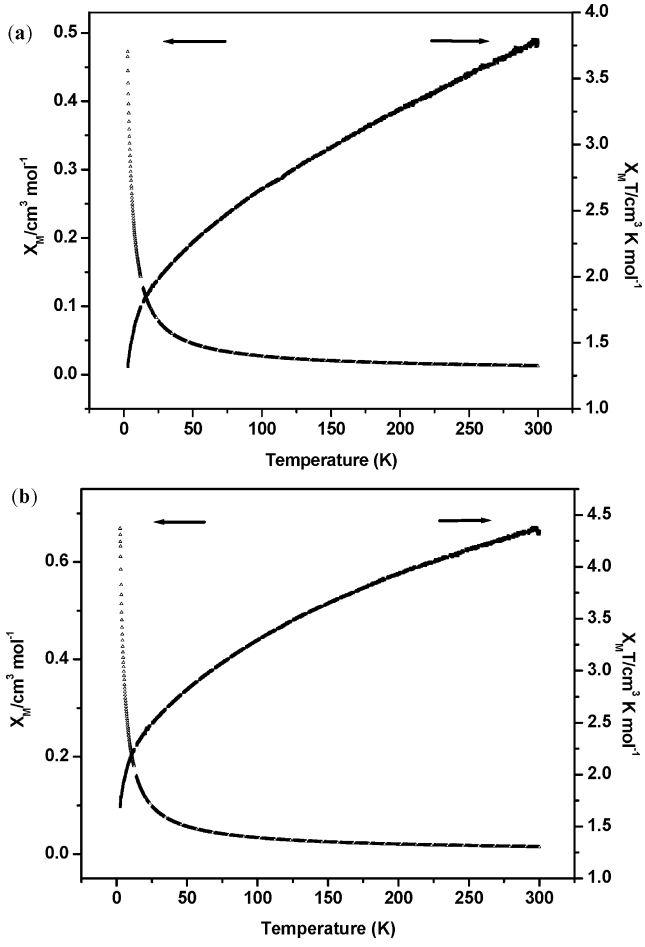

Figure 11. Temperature dependences of χ_M (Δ) and $\chi_M T$ (◆): (a) $[\{Sm(H_2O)_6\}_2As_8V_{14}O_{42}(SO_3)]\cdot 8H_2O$ (**2**) and (b) $[\{Ce(H_2O)_6\}_2As_8V_{14}O_{42}(SO_3)]\cdot 8H_2O$ (**3**).

μ_B; 0.09 cm^3 K mol^{-1}) at 298 K.[19] For compound **2**, if we add the room temperature (experimental) contribution from the Sm^{3+} ion (e.g., 1.6 μ_B; 0.32 cm^3 K mol^{-1} per Sm^{3+}) to the experimentally obtained room temperature $\chi_M T$ value of discrete compound $[NH_4]_6[As_8V_{14}O_{42}(SO_3)]$ (2.48 cm^3 K mol^{-1}; 4.45 μ_B),[8a] the resulting calculated $\chi_M T$ value of 3.12 (2.48 + 0.32 + 0.32) cm^3 K mol^{-1} is somewhat smaller than the experimentally obtained $\chi_M T$ value (3.76 cm^3 K mol^{-1}) of samarium compound **2** at room temperature, indicating a weak interaction between the linkers (Sm^{3+} ions) and V(IV) centers of the $\{V_{14}\}$cluster anion at room temperature.

In the case of the Ce^{3+} ion, the theoretical value of μ_J (2.54 μ_B; 0.806 cm^3 K mol^{-1}) agrees nicely with experimental value of μ_{obsd} (2.3−2.5 μ_B) at room temperature.[19] For compound **3**, if we add twice this corresponding $\chi_M T$ value 1.61 (0.806 + 0.806) cm^3 K mol^{-1} to the experimentally obtained room temperature $\chi_M T$ value of discrete compound $[NH_4]_6[As_8V_{14}O_{42}(SO_3)]$, the resulting $\chi_M T$ value of 4.09 (1.61 + 2.48) cm^3 K mol^{-1} is again somewhat smaller than the experimentally obtained $\chi_M T$ value (4.35 cm^3 K mol^{-1}) of cerium compound **3** at room temperature, suggesting again a week interaction between the Ce^{3+} ion ($4f^1$) and the V^{4+} ion ($3d^1$) at room temperature.

As the temperature decreases, both compounds **2** and **3** exhibit identical trends in magnetic behavior, as shown by Figure 11a and b, respectively. For both compounds, as the temperature decreases, the $\chi_M T$ value continuously decreases (in contrast to the temperature-dependent magnetic behavior of discrete compound $[NH_4]_6[As_8V_{14}O_{42}(SO_3)]$ as discussed below), reaching a value of 1.99 cm^3 K mol^{-1} (compound **2**) and 2.50 cm^3 K mol^{-1} (compound **3**) at 25 K; below this temperature, the $\chi_M T$ value decreases very rapidly, reaching 1.33 cm^3 K mol^{-1} (for compound **2**) and 1.71 cm^3 K mol^{-1} (for compound **3**) at 2.8 K. This magnetic behavior indicates overall antiferromagnetic coupling interactions (see Figure 11a and b). Since the trends in magnetic behavior for both compounds **2** and **3** are alike, the coupling interactions between Sm^{3+}/Ce^{3+} and V^{4+} ions of the $\{V_{14}\}$ cluster anion can be ignored while the temperature decreases. If there would exist significant interaction between lanthanide ions (Sm^{3+}/Ce^{3+}) and V^{4+} ions of the $\{V_{14}\}$ cluster anions, we would not have observed identical trends in temperature-dependent magnetic behavior, because the Ce^{3+} ion is an f^1 system (one unpaired electron) and Sm^{3+} ion is an f^5 system (five unpaired electrons). The insignificant coupling interactions between lanthanide ions (Sm^{3+}/Ce^{3+}) and V^{4+} ions of $\{V_{14}\}$ cluster anions with decreasing temperature can also be supported by the fact that the $\chi_M T$ value for the discrete compound $[NH_4]_6[As_8V_{14}O_{42}(SO_3)]$ is 1.78 cm^3 K mol^{-1} at 2 K[8a] and the $\chi_M T$ values for compounds **2** and **3** are 1.33 cm^3 K mol^{-1} and 1.71 cm^3 K mol^{-1}, respectively, at 2 K. The theoretical values of $\chi_M T$ for compounds **2** and **3** are 1.96 (1.78 + 0.09 + 0.09) cm^3 K mol^{-1} and 3.39 (1.78 + 0.806 + 0.806) cm^3 K mol^{-1}, respectively, at 2 K. This clearly indicates that the sources of antiferromagnetic coupling interactions that are revealed from Figure 11a and b with decreasing temperature for both compounds **2** and **3** are solely the $\{V_{14}\}$ cluster with 14 V^{4+} ions and inter-$\{V_{14}\}$ cluster interactions that are possible due to lanthanide linking (see Figure 4). The magnetic behavior of compounds **2** and **3** is in contrast to the temperature-dependent magnetic

(19) Dutta, R. L.; Syamal, A. *Elements of Magnetochemistry*, 2nd ed.; East-West Press Pvt. Ltd.: New Delhi, India, 1993.

behavior of the discrete compound $[NH_4]_6[As_8V_{14}O_{42}(SO_3)]$, for which the room temperature $\chi_M T$ value is 2.48 cm^3 K mol^{-1} (4.45 μ_B). As the temperature decreases, the $\chi_M T$ decreases slightly, stabilizing at 2.1 cm^3 K mol^{-1} at around 100 K. Subsequently, the $\chi_M T$ value increases with decreasing temperature, reaching a maximum of 2.3 cm^3 K mol^{-1} at 15 K. Finally, below 10 K, the $\chi_M T$ value of $[NH_4]_6[As_8V_{14}O_{42}(SO_3)]$ decreased rapidly, reaching 1.78 cm^3 K mol^{-1} at 2 K.[8a] This suggests that assembling $\{V_{14}\}$ clusters has tremendous influence on the magnetism of the discrete cluster irrespective of the type of linker. For compound $[\{La(H_2O)_6\}_2As_8V_{14}O_{42}(SO_3)]\cdot 8H_2O$ (**1**), there is no contribution to the magnetic susceptibility from the La^{3+} ion (f^0 system), and thus, the room temperature $\chi_M T$ value (2.35 cm^3 K mol^{-1}) of **1** is comparable to that (2.48 cm^3 K mol^{-1}) of discrete compound $[NH_4]_6[As_8V_{14}O_{42}(SO_3)]$.[8a] However, the temperature-dependent magnetic behavior of compound $[\{La(H_2O)_6\}_2As_8V_{14}O_{42}(SO_3)]\cdot 8H_2O$ (**1**), which shows a continuous deccrease in $\chi_M T$ values with decreasing temperature, indicating overall antiferromagnetic coupling interactions, is not comparable to the reported magnetic behavior of the discrete starting precursor $[NH_4]_6[As_8V_{14}O_{42}(SO_3)]$[8a] (see the Supporting Information for magnetic details of compound **1**, Figure S8). This, again, tells us that it is linking (not the type of linker) that plays a key role in affecting the magnetism of the discrete cluster, when it is linked to an extended structure. We believe that the linking of the $\{V_{14}\}$ clusters by lanthanide ions probably provides a pathway for exchange interactions among $\{V_{14}\}$ clusters, resulting in strong antiferromagnetic interactions, as is evidenced by the continuous decrease of the $\chi_M T$ values with decreasing temperature (Figure 11). This also explains why the room temperature $\chi_M T$ value for the linked system **1** is slightly smaller that that of discrete system $[NH_4]_6[As_8V_{14}O_{42}(SO_3)]$.[8a] Recent literature reports also support these intercluster antiferromagnetic interactions.[9]

For both compounds **2** and **3**, the appearance of the rapid decrease of the $\chi_M T$ value (see Figure 11a and b) between 25 and 2 K is an indication of a different exchange pathway, which is difficult to explain at this stage without fitting the data to a suitable model. Unfortunately, it is not easy to fit the experimental magnetic data for compounds **1**, **2**, and **3** using a suitable theoretical model.[20] For this isolated discrete cluster containing compound $[NH_4]_6[As_8V_{14}O_{42}(SO_3)]$, the experimental value of $\chi_M T$ at lower temperatures agreed with a ground state of $S = 1$.[8a] The present experimental data for compounds **2** and **3** also agrees with an $S = 1$ ground state that gets populated at the lowest temperature.

Thermal Studies: How Linking of the POV Cluster Anion with Lanthanide−Aqua Complex Cations Offers Extra Stability. The thermogravimetric analyses of all compounds were performed in flowing N_2 with a heating rate of 5 °C min^{-1} in the temperature range 30−1100 °C. The discrete cluster $[NH_4]_6[As_8V_{14}O_{42}(SO_3)]$ (starting precursor) was synthesized from the reported procedure,[7a] and the TG curve of this shows the first weight loss of 5.18%, which corresponds to the loss of six ammonium cations per formula unit in the temperature range 35−134 °C (calculated mass loss for six ammonium ions is 4.97%). The major loss observed in the temperature range of 480−520 °C is due to the removal of encapsulated SO_3 molecule as SO_2 gas, followed by the cluster decomposition. The evolution of SO_2 gas at this temperature is evidenced by the thermogravimetric analysis (TGA)/mass curve, as shown in Figure 12a. The TGA/mass curve for compound $[\{La(H_2O)_6\}_2As_8V_{14}O_{42}(SO_3)]\cdot 8H_2O$ (**1**) is shown in Figure 12b. This can be divided into four stages. The first weight loss of 5.27% is assigned due to the loss of eight lattice water molecules (see formula of compound **1**) in the temperature range 35−128 °C (calculated mass loss is 5.33% for eight water molecules). The observed second weight loss of 8.49% should be due to the loss of 12 lanthanum-coordinated water molecules that occurs in the temperature range of 128−500 °C (calculated mass loss is 7.99% for 12 water molecules). The third and fourth mass losses of 25.25% and 9.41%, respectively, in the temperature range of 500−1050 °C are due to the decomposition of encapsulated sulfurtrioxide (as exclusion of SO_2 gas) and $\{V_{14}\}$ cluster decomposition, respectively. The identification of sulfur dioxide was elucidated by the mass of SO_2 gas in the TGA/mass curve (Figure 12b) that particularly occurs in the temperature range of 520−580 °C.

Thus, in compound **1**, the structure decomposition is observed in the temperature range 520−580 °C, but the same decomposition of the discrete ammonium cluster occurs in the temperature range 480−520 °C. We believe that this elevation in the decomposition temperature of compound **1** (in comparison with discrete cluster compound) has been achieved because of the following reasons: (i) compounds **1**−**3** are organic free framework materials; (ii) in the framework, each cluster anion exhibits hexa-coordination with its surrounding six different lanthanum cations, leading to a two-dimensional coordination polymer that offers extra stability to the $\{V_{14}\}$ cluster anion; (iii) the cluster anion is involved in forming a supramolecular hydrogen-bonded three-dimensional network that also provides extra thermal stability; (iv) the encapsulated sulfurtrioxide anion, which is found to interact with the inner wall of the cluster anion, may offer more rigidity to the cluster anion.

In order to check whether the first two weight losses in the TG curve (Figure 12) are due to the loss of water molecules, we performed TG experiments with preheated samples of compound **1**. The sample, obtained by heating at 200 °C for 3 h, shows a first loss 6.12% in the temperature range 35−176 °C that corresponds to the loss of nine water molecules per formula unit (calculated mass loss is 5.99% for nine water molecules). We believe that these water molecules are lanthanum-coordinated water molecules. There is a total of 12 lanthanum coordinated water molecules per formula unit; probably, three of these got lost with solvent water molecules from the crystal lattice during preheating at 200 °C. The second and third losses of 19.26% and 3.01% are due to the loss of the encapsulated sulfurtrioxide molecule (as SO_2 gas) followed

(20) Khan, O. *Molecular Magnetism*; VCH: Weinheim, Germany, 1993.

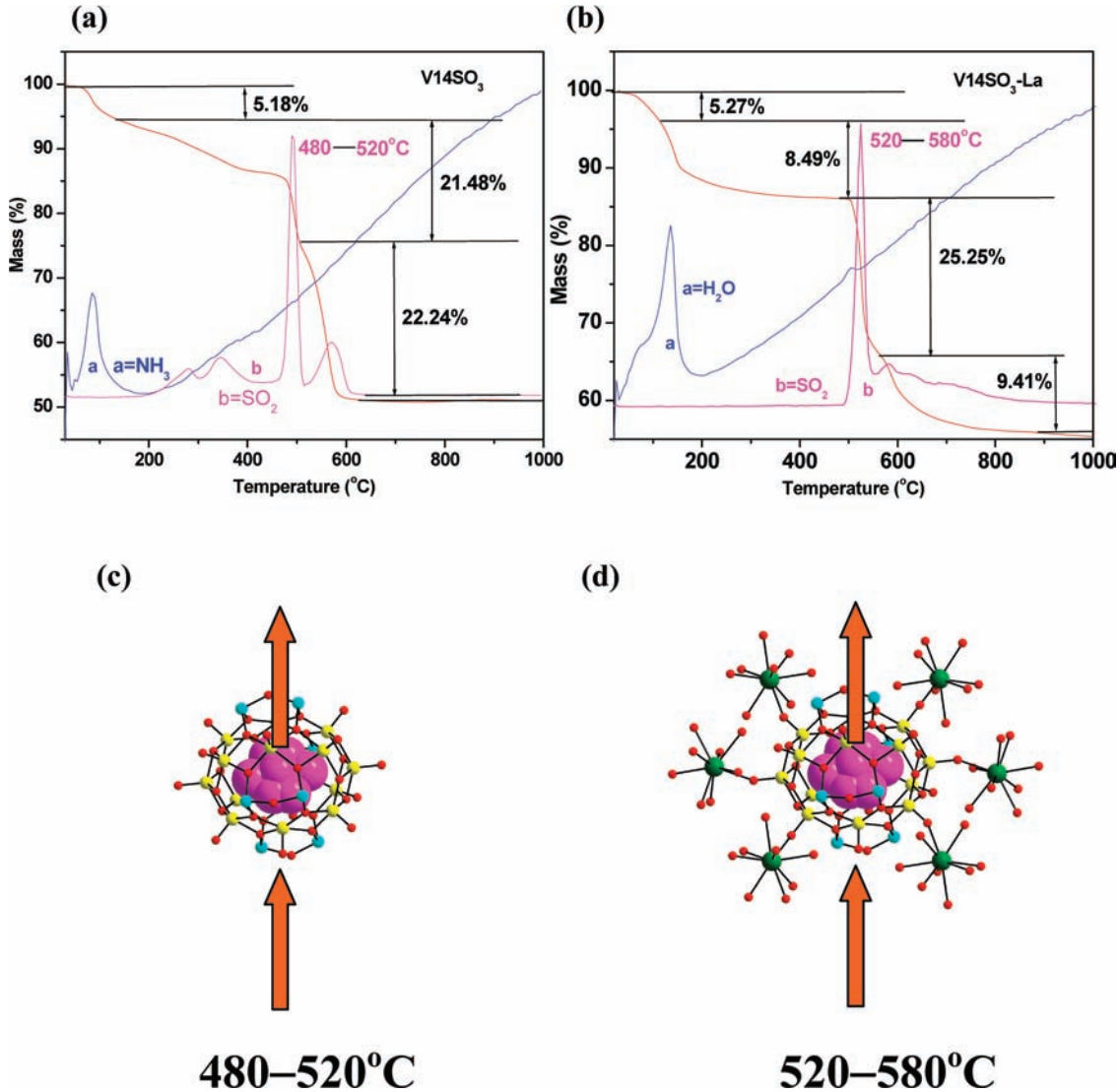

Figure 12. (a) TGA/mass plot of the starting precursor $[NH_4]_6[As_8V_{14}O_{42}(SO_3)]$. (b) TGA/mass plot of the compound $[\{La(H_2O)_6\}_2As_8V_{14}O_{42}(SO_3)]\cdot 8H_2O$ (**1**). (c) The pictorial representation of the evolution of sulfur trioxide (as exclusion of SO_2 gas), which is encapsulated in the cavity of the cluster anion, $[As_8V_{14}O_{42}]^{4-}$, in the starting precursor $[NH_4]_6[As_8V_{14}O_{42}(SO_3)]$. (d) The schematic representation of the evolution of sulfur trioxide (as exclusion of SO_2 gas), which is encapsulated in the cavity of the cluster anion, $[As_8V_{14}O_{42}]^{4-}$, in compound $[\{La(H_2O)_6\}_2As_8V_{14}O_{42}(SO_3)]\cdot 8H_2O$ (**1**).

by the structural decomposition. The corresponding TGA graph is shown in Figure 13a.

The preheated sample at 400 °C for 3 h shows the weight loss in two steps. The first loss of 17.83% in the temperature range 450−580 °C is due to the loss of encapsulated SO_3^{2-} (confirmed by the mass of released SO_2 gas), and the second loss of 8.34% is due to the cluster decomposition. The relevant TGA graph is shown in Figure 13b. The compounds **1**−**3** are isostructural and hence show the identical TGA/mass spectra and exhibit similar types of weight losses (see the Supporting Information for the TGA/mass curves for compounds **2** and **3**). Thus, thermogravimetric analysis indicates that this series of compounds has a significant amount of thermal stability in the solid state.

Sulfite Anion: Inclusion versus Exclusion. In the present series of compounds **1**−**3**, the sulfite anion is found to be completely encapsulated in the cavity of the cluster anion $[As_8V_{14}O_{42}]^{4-}$, giving rise to a sulfite-encapsulated cluster anion $[As_8V_{14}O_{42}(SO_3)]^{6-}$. It would be interesting to see how a metal-oxide-based rigid cluster cage protects the encapsulated guest against an external force, for example, thermal energy. Although anion inclusion in the cavity of a POV cluster anion has been long known, so far, no attempts have been made to explore the stability of an anion in terms of its inclusion versus exclusion. As shown in Figure 12, the decomposition of encapsulated sulfurtrioxide is found to occur in the temperature range of 480−520 °C for the discrete cluster anion and 520−580 °C for linked system (vide supra). In order to understand the role of the cluster cage in protecting its incorporated sulfite anion against high temperatures, we performed TGA/mass studies of bare $NaHSO_3$. As shown in the TGA/mass plot of bare $NaHSO_3$ (Figure S7, Supporting Information, section S5), a complete loss of sulfite as SO_2 gas is found to occur in the temperature range 190−320 °C. This clearly indicates that the POV cluster anion $[As_8V_{14}O_{42}]^{4-}$ offers substantial protection toward its encapsulated sulfite anion.

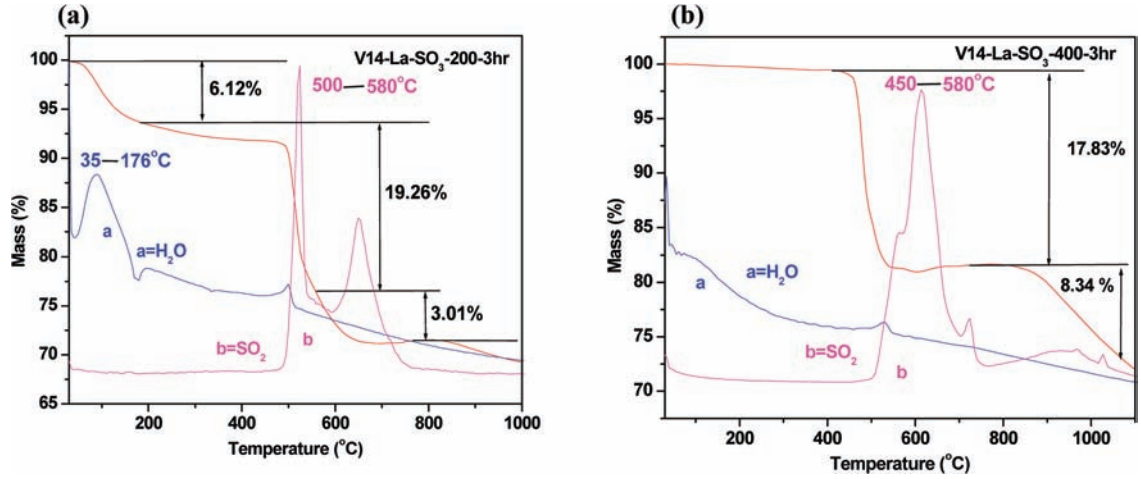

Figure 13. TGA/mass plot of preheated compound **1** (a) at 200 °C/3 h and (b) at 400 °C/3 h. Color code: TGA curve, red line; water mass loss curve, blue line; sulfurdioxide mass loss curve, purple line.

Conclusion

Even though, this particular POV cluster anion $[As_8V_{14}O_{42}]^{4-}$ has been extensively studied in the context of magnetism, its linking propensity is not explored to that extent. The coordination polymers, reported earlier on the basis of this POV cluster anion, were synthesized using transition metal coordination complexes (as linkers) with organic fragments as chelating ligands.[9] Organic free extended structures with this POV building unit, which would be a more stable system in a materials sense, have not yet been explored. We have used hexa-aqua−lanthanide complexes, $[Ln(H_2O)_6]^{3+}$ (Ln = La^{3+}, Sm^{3+}, and Ce^{3+}) as a linker in constructing a new class of organic free coordination polymers $[\{Ln(H_2O)_6\}_2As_8V_{14}O_{42}(SO_3)]\cdot 8H_2O$, Ln = La^{3+} (**1**), Sm^{3+} (**2**), and Ce^{3+} (**3**), that can be isolated in a controlled reaction setup starting from an ammonium salt of this POV cluster $[NH_4]_6[As_8V_{14}O_{42}(SO_3)]$ and $Ln(NO_3)_3\cdot 6H_2O$. To the best of our knowledge, this is the first example of a V/As/O system-based coordination polymer that uses a lanthanide complex as a linker to construct this class of extended structures. We have shown that the POV cluster anion is attached to its surrounding six $[Ln(H_2O)_6]^{3+}$ coordination complexes by coordinate covalent bonds, which is very rarely described in polyoxometalate chemistry. This hexa-coordination of a POV cluster anion, demonstrated here, represents the rare example of a POV cluster of this kind.

We have shown how linking a very well known and well studied magnetic object[8] $[As_8V_{14}O_{42}(SO_3)]^{6-}$ influences its magnetism. It has been demonstrated that the antiferromagnetic coupling interactions increase in the case polymeric system (compounds **1**, **2**, and **3**) compared to its discrete analogue. We have proposed that intercluster $V^{4+}-V^{4+}$ interactions are responsible for the increase in antiferromagnetic coupling interactions in these linked systems.

This work has an important implication for the conversion of a discrete POV cluster anion into a two-dimensional framework, formed by a coordinate covalent bond that further extends to three-dimensional networks using supramolecular hydrogen-bonding interactions. The TGA/mass analysis of the present system has been discussed elaborately. We have demonstrated that the structural decomposition temperature of this new class of coordination polymers has been elevated significantly, compared with that of the discrete cluster compound, $[NH_4]_6[As_8V_{14}O_{42}(SO_3)]$. We have demonstrated how a metal-oxide-based cluster cage influences the stability of an inorganic anion, when it is encapsulated in the cavity of that cluster anion. This offers us the possibility to carry an inorganic anion (through its inclusion) to an environment of a higher-temperature zone where the inorganic anion is otherwise unstable. The present work provides a novel synthetic route to obtain a new group of metal-oxide-based networks of a very important magnetic object.

Acknowledgment. We thank the Department of Science and Technology, Government of India, for financial support (Project No. SR/SI/IC-23/2007). We are thankful to Professor M. V. Rajashekaran and Dr. R. Chandrasekar for helping us in analyzing magnetic susceptibility data. Special thanks are due to Professor A. R. Chakravarty and Mr. Pijus K. Sasmal of the Indian Institute of Science, Bangalore, for providing the variable-temperature magnetic susceptibility data for compounds described in the manuscript. We also thank Dr. Tapas K. Maji (Jawaharlal Nehru Centre for Advanced Scientific Research, Bangalore) for providing the variable-temperature magnetic susceptibility data for compounds **2** and **3** between 2 and 300 K. The National X-Ray Diffractometer facility at the University of Hyderabad under the Department of Science and Technology, Government of India, is gratefully acknowledged. We thank Shafy from DMRL (Hyderabad) for helping us in providing the ICP data. T.A. thanks CSIR, Government of India, for a fellowship. This work is dedicated to Eminent Professor C. N. R. Rao on the occasion of his 75th birthday.

Supporting Information Available: Tables of bond distances and angles for compounds **1**, **2**, and **3** and a table of hydrogen-bonding parameters for compound **1**; ESR figures; X-ray powder diffraction patterns (observed and simulated single crystal data); TGA plots for compounds **2** and **3**; bond valence sum calculations; variable-temperature magnetic data for compounds **1**, **2**, and **3**; and X-ray crystallographic files in CIF format for compounds **1**, **2**, and **3**. This material is available free of charge via the Internet at http://pubs.acs.org.

IC8002383